J. Fluid Mech. (2011), *vol.* 682, *pp.* 397–414.
doi:10.1017/jfm.2011.230

Occlusion criteria in tubes under transverse body forces

ROBERT MANNING[1], STEVEN COLLICOTT[1] AND ROBERT FINN[2]†

[1]School of Aeronautics and Astronautics, Purdue University, W. Lafayette, IN 47907, USA

[2]Mathematics Department, Stanford University, Stanford, CA 94305-2125, USA

(Received 26 August 2010; revised 29 April 2011; accepted 13 May 2011; first published online 13 July 2011)

When a fluid in a tube is occluded, one finds a static configuration in which the occluding free surface of the fluid is an equilibrium capillary surface spanning the tube. We extend known criteria for existence and non-existence of such a surface, leading to an explicit mathematically rigorous occlusion criterion for cylindrical tubes in a transverse body force field, depending on the force magnitude and contact angle. For any contact angle $\gamma \neq \pi/2$, we provide further an explicit design of a tube section, which will not occlude in a downward gravity field, regardless of the field strength. In addition, we derive a precise analytic occlusion criterion for liquid partially filling a circular vessel spinning about its axis.

Key words: drops and bubbles, gas/liquid flow, interfacial flows, microfluidics

1. Introduction

Both interfacial and body forces play important roles in determining the shape of the interface between two fluids under static conditions. In a cylinder of arbitrary cross-section, a variety of interface configurations may exist under weightless conditions, which may or may not occlude or block the entire cross-section (Collicott, Lindsley and Frazer 2006). If a body force is then applied, blockage may or may not occur, depending on the force and on how it is applied. Predicting the conditions when occlusion of the cylinder or vessel may occur can be of value for a variety of applications.

Mechanical and fluid systems can often, in principle, be miniaturized, towards obtaining benefits similar to those achievable in the current microelectronics industry. Lab-on-a-chip technology may replace a series of bench-top instruments with a single, low-cost, disposable medical device (Zoval & Madou 2004). Miniaturization of fluid systems can, however, lead to new challenges, one of which is the eventual formation of liquid plugs or gas bubbles in channels. In larger systems, such plugs do not generally form, as bubbles will block only a small portion of the channel and may be advected downstream. However, in smaller devices, the bubble or liquid volume may occlude or block the entire cross-section of the channel. This may reduce performance or may even damage the system. Such liquid plugs are known to occur in fuel cells (Zhang, Yang & Wang 2006; Litterst *et al.* 2006), micro-electrical mechanical systems (MEMS) (Gravesen, Branebjerg & Jensen 1993), and other devices. Predicting the

† Email address for correspondence: finn@math.stanford.edu

formation of these bubbles or liquid plugs is an essential step towards creating more reliable or efficient MEMS and fuel cells.

Vane-type propellant management devices are metal structures that are used to position liquid propellant within a satellite fuel tank when in micro-gravity. These vanes are thin metal plates that are inside of and perpendicular to the tank wall. In practice, the vane and outer wall are not in contact and have a small separation gap. For no separation gap, a liquid with a contact angle of less than 45° will always wet the corner formed along the vane and vessel wall (Concus & Finn 1969). For small separations, the liquid will fill the gap if the liquid contact angle and gap separation are small enough (Chen & Collicott 2006). Thus, some liquid is guaranteed to be between the vanes and tank wall. While the liquid will nominally be under micro-gravity, station keeping and momentum dump manoeuvres can introduce transverse accelerations which may disturb the liquid orientation. If the acceleration is too large, the liquid will recede from the vane structure and may cause a disruption in propellant flow.

Zoological and phytological disciplines may also benefit from understanding the gravitational effects on a gas–liquid interface in a channel. For example, air embolism occurs when cardiovascular vessels intake air bubbles and may result in death. Gravitational forces, surface tension and forces due to the flow play a role in determining the bubble shape and behaviour (Bull 2005).

The above examples illustrate the importance of understanding the quantitative configuration of the equilibrium gas–liquid interface under a gravitational field. For MEMS and fuel cells, can a liquid form a plug that will occlude the channel? For propellant management devices, will the liquid wet the entire vane structure? What vessel size will allow gas bubbles to obstruct the flow? We obtain here answers to some of these questions in physically relevant contexts by adapting a general existence/non-existence theory for capillary surfaces developed by (Finn 1986).

We emphasize that all material of this paper is based on rigorous mathematical theory, not on approximations. This can be important, as the highly nonlinear nature of the problem makes it difficult to estimate the consequences of approximating the equations.

2. Previous work

Capillarity in small vessels was apparently initially described by Leonardo da Vinci about 1500. The first successful quantitative descriptions were achieved in the early 19th century by Young and by Laplace. General existence theorems have appeared during the past half century (see, e.g. Finn 1975 for citations). Non-existence theorems are significant in this theory, and serve to distinguish the two kinds of surfaces indicated in figure 1. The general criterion was developed by Finn (1986) for capillary surfaces under weightlessness or force fields directed along the z-axis. The non-existence criterion of Finn (1986) extends immediately to any force field, regardless of direction, and provides our criterion for the absence of an occluding surface. Smedley (1990) and Chen & Collicott (2006) have already applied the criterion of Finn (1986) to several vessel cross-sections under weightlessness. The criteria change in essential qualitative ways when force fields are introduced, and the results of the present work reflect those distinctions.

While an extensive literature is devoted to weightless states, the literature on bounded capillary interfaces is much more limited when a body force is included. Jensen *et al.* (1987) studied the effect of gravity on a two-dimensional Hele–Shaw cell.

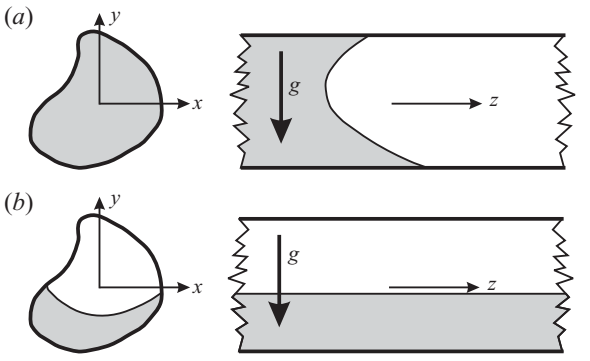

FIGURE 1. (*a*,*b*) Two possible interface configurations.

However, many practical vessels and channels, including those mentioned above, are not two-dimensional and have a finite width. DeLazzer *et al.* numerically calculated the capillary pressure in a rotating polygonal cylinder (de Lazzer *et al.* 1996). They noted that a bifurcation of the interface shape exists at a particular rotation rate. Later, deLazzer *et al.* examined lateral acceleration of liquids pinned between two parallel plates (de Lazzer *et al.* 2003).

The behaviour of liquids partly filling tubes in the presence of transverse gravity fields has apparently not been studied explicitly from a theoretical point of view; however, the theory developed by Finn (1986) for the case of fields parallel to the generators can be adapted to the needs of the present study. Of particular interest for us is the dichotomy that appears, between existence and non-existence of surfaces satisfying the prescribed geometrical conditions; see, for example, Concus & Finn (1990) for background discussion. We base the present work on the observation that the *existence of a capillary surface interface in the sense indicated in Finn* (1986) *expresses physically the possibility of occlusion by an equilibrium interface; correspondingly, the non-existence criterion analogous to that indicated in Finn* (1986) *guarantees that no occluding interface can form.* We develop those criteria in the ensuing §§ 3 and 4. In § 5, we apply the theory to the simplest case of tubes with circular section. In this event, occluding surfaces for vanishing external field are known explicitly as spherical caps. We show that with increasing (uniform) transverse field strength, occlusion persists up to a critical field strength (expressed non-dimensionally by 'Bond number' B), above which it cannot occur and the fluid configuration changes dramatically – in general in a discontinuous way – to a configuration not blocking the tube. As a check on our procedure, we evaluated the critical $B = B_0$ in two independent ways, (*a*) as direct consequence of the theory just indicated, and (*b*) by searching empirically for surfaces of minimizing energy, via the Brakke 'Surface Evolver' (Brakke 2011). The comparison of results, as displayed in figure 4, is we think convincing.

In general, occlusion of flow in tubes is a highly complex dynamical phenomenon, which we do not attempt to describe here. Once occlusion occurs, the configuration becomes static. Ultimately, one wants to know when that can occur and to describe to the extent feasible the shape of the occluding surfaces S. In actual flow through tubes, there will be a driving pressure from a 'pumping station' far upstream, imposing a force directed along the tube in the flow direction. When occlusion occurs, there remains a uniform pressure jump across S, which may differ from the pressure jump

predictable from the contact angle condition and which must be accounted for in determining the configuration. In principle, this term is accessible to our method, and we plan to include it in a future work. In the present initial effort, we restrict attention to stationary configurations in the absence of external forces. In this sense, our material is directly in the stream of earlier numerical investigations by Reynolds & Satterlee (1966) and by Concus (1968), and experimental studies by Derdul, Masica and Petrash (1964), and by Masica (1967).

The earlier of these studies were directed to free surfaces S of cylindrical fluid columns with circular section subject to (gravitational) body forces directed along the cylinder axis. In Reynolds & Satterlee (1966) and in Concus (1968), the symmetric solutions were characterized numerically, up to a critical 'Bond number' $B_0(\gamma)$ at which (symmetric) stability failed. Notably, the value $B_0(0) = 0.842$ was established. The reference Derdul *et al.* (1964) examined the question experimentally for varying combinations of physical parameters, with a determination $B_0(0) = 0.84$ in all cases, a remarkable confirmation of the formal theory.

Masica (1967) repeated earlier experiments in an extensive and carefully controlled investigation, replacing the axial field with a transverse field, as studied in the current work. He asserted a value $B_0(0) = 1.25 \pm 0.05$. This can be compared with the present theoretical prediction, in § 5 of the present work, of $B_0(0) = 1.01$. We are inclined to ascribe the discrepancy to difficulties in exact determination of contact angle. The experimental value 1.25 is attained theoretically at $\gamma = 4.57°$.

There are basic conceptual differences, distinguishing the procedure underlying the present work from that in Reynolds & Satterlee (1966) and in Concus (1968). The earlier references are based on linearizing perturbations of the implicitly known symmetric solutions, and offer no guaranty that independent surfaces of lower energy have not been overlooked. Additionally, they are based on explicit knowledge of individual solutions. The present work is based on a general (lower dimensional) criterion introduced by Finn for existence or for non-existence of a surface spanning the cylinder walls and minimizing the free energy of the system (see Finn 1986, Chap. 7). The non-existence criterion is elementary, and provides directly an explicit test for excluding occlusion. The general theory, as developed in Finn (1986), shows that in the (dichotomous) situation for which the test fails, an occluding surface does, in fact, exist. Since in this theory, existence is obtained via an energy minimizing procedure, and since the second variation is strictly positive, we are assured *ab initio* that occluding surfaces determined by the procedure are stable.

The theory as offered in Finn (1986) determines when occlusion can occur, but provides no information on the shape of the occluding surface when it exists. To this and related purposes, we have relied on the Brakke surface evolver software (SE), which computes surfaces described by a minimal energy procedure and bound by various constraints. The surface is modelled as a union of triangles and is found by using a gradient descent method (Brakke 2011). Each iteration evolves the surface to a lower energy state than the prior surface. By successively iterating the surface, one can achieve in many situations an excellent approximation to the lowest energy state. The iterations are computational steps and do not represent any physical process. The surface can also be dynamically adjusted by adding facets, smoothing the surface and other functions. While SE is designed to find three-dimensional equilibrium interfaces for a particular set of conditions, it can be used to determine the range of parameters for which a surface exists. However, one must take precautions to ensure an accurate result. For an occluding surface without gravity, the free surface must be tessellated by several thousand triangular facets in conjunction with a special evolution scheme

(Collicott & Weislogel 2004). Several hours of computation time may be required to obtain an accurate result.

The first formal criterion for non-existence is apparently due to Concus & Finn (1969) for a section Ω of particular form. The criterion of Concus & Finn (1969) was extended to cylinders of general cross-section by Finn (1986). In outline, we follow the procedures developed in Finn (1986); however, instead of the body force parallel to the cylinder generators contemplated in that reference, we consider a transverse force orthogonal to the generators. Although this situation is not formally covered in Finn (1986), the extension requires only perfunctory changes in the proof. As must be expected, the specific criteria encountered adopt a significantly different structure than occurs with axially directed forces.

3. Problem defined

We consider a rigid vessel with a fixed cross-section Ω, as shown in figure 1. The vessel cross-section in the x-y plane is of arbitrary shape. The length of the vessel along the z direction is assumed infinite. The vessel is composed of a homogeneous material, and temperature is assumed temporally and spatially constant. The vessel contains two different fluids of different densities ρ_1 and ρ_2. Only the difference in densities (taken as positive) is significant for us; we denote it by ρ. Both fluids have very large fixed volumes and are immiscible with respect to one another. The interface has a fixed surface tension coefficient σ and meets the wall at a uniform contact angle γ. We restrict attention to equilibrium configurations with fixed γ. Dynamic contact angle behaviour or hysteresis depends on the motion or previous state of the free surface, which are not considered in this analysis.

A constant body force, due to a lateral acceleration or gravity, may be applied. The body force is to be aligned with the y-direction and thus has no axial component in the z-direction. The system is in mechanical equilibrium, and multiple static configurations may exist, in each of which both fluids cover the indicated base domains. The fluid may occlude the entire cross-section of the vessel with a smooth surface $z = u(x, y)$ meeting the channel walls in the prescribed angle γ, as shown in figure 1(a). Alternatively, there may exist a *soluzione generalizzata* (Giusti 1984) for which $u(x, y) \equiv \infty$ over a domain of positive area, as shown in figure 1(b). The former case corresponds to occlusion by the surface $u(x, y)$. In the latter case, the surface extends cylindrically to infinity in both directions along the channel. The (lower) infinite domain it bounds can be filled with liquid in equilibrium. In principle, one would expect that the fluid could be moved (sufficiently slowly) almost rigidly in the direction of the generators through any given portion of that region, to obtain a flow without occlusion. However, we have not proved that.

As in figure 1, we adopt coordinates (x, y, z) with z along the generator. When the interface can be expressed in the form $z = u(x, y)$, the capillary equation is the following (Finn 1986):

$$\nabla \cdot (Tu) = 2H(x, y, u), \quad \text{with } Tu \equiv \frac{\nabla u}{\sqrt{1 + |\nabla u|^2}}. \tag{3.1}$$

Here, H is the mean curvature of the surface. In the classically considered case in which a gravity field g is directed downwards across a fluid surface $u(x, y)$, it follows from laws of hydrostatics (Finn 1986) that $2H = \lambda + \kappa u$, where $\kappa = \rho g/\sigma$. Here λ is a constant depending on eventual volume constraint, ρ is the density change

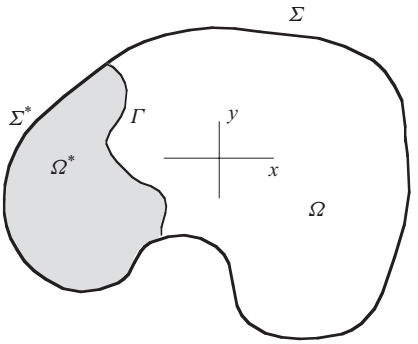

FIGURE 2. General section $\Omega : z = c$ of cylindrical tube, showing arc Γ subtending subdomain $\Omega^* \subset \Omega$ and arc $\Sigma^* \subset \Sigma$.

across the surface and σ the surface tension. The analogous procedure in the present configuration yields

$$2H = \lambda + \kappa y. \tag{3.2}$$

In all cases, the liquid meets the tube wall at a prescribed contact angle γ, depending only on the materials. Thus, along the boundary Σ of a base domain (orthogonal section) Ω, there holds

$$\nu \cdot Tu = \cos\gamma, \tag{3.3}$$

where $\boldsymbol{\nu}$ is unit exterior normal to the tube on Σ. If the materials are homogeneous, then γ will be constant, as we shall assume. An occluding surface in the tube would appear as an interface that must satisfy (3.1) and (3.2) over Ω and (3.3) over Σ. This corresponds to a plug through which no fluid can pass. We may restrict attention to occluding surfaces that are graphs $z = u(x, y)$ over Ω, as Vogel (1988) showed that to be the only possibility. We suppose the existence of such an interface and follow the general line of approach indicated in Finn (1986), Chap. 7. We choose the constant λ so that the centroid of Ω lies on the line $y = 0$. Using the above relations, we then obtain

$$\lambda = \frac{|\Sigma|}{|\Omega|}\cos\gamma, \int_\Omega y \,\mathrm{d}x\,\mathrm{d}y = 0. \tag{3.4}$$

We now integrate (3.1) over a general subdomain $\Omega^* \subset \Omega$, bounded in part by a curve $\Gamma \subset \Omega$ and subtending an arc $\Sigma^* \subset \Sigma$ (see figure 2).

We find, using (3.3) on Σ^* and (3.2) and (3.4) in Ω^*

$$\int_{\Omega^*} \operatorname{div} Tu \,\mathrm{d}x\,\mathrm{d}y = |\Sigma^*|\cos\gamma + \int_\Gamma \nu \cdot Tu \,\mathrm{d}s = \frac{|\Sigma|}{|\Omega|}|\Omega^*|\cos\gamma + \kappa\int_{\Omega^*} y \,\mathrm{d}x\,\mathrm{d}y. \tag{3.5}$$

The crucial observation is that for any differentiable function $u(x, y)$, there holds $|Tu| < 1$. As a consequence, both (3.6) and (3.7) must hold for all smooth $\Omega^* \subset \Omega$ for which $\Omega^* \neq \emptyset, \Omega$

$$\Phi\left[\Omega^*\right] \equiv |\Gamma| - |\Sigma^*|\cos\gamma + \frac{|\Sigma|}{|\Omega|}|\Omega^*|\cos\gamma + \kappa\int_{\Omega^*} y \,\mathrm{d}x\,\mathrm{d}y > 0, \tag{3.6}$$

$$\Psi\left[\Omega^*\right] \equiv |\Gamma| + |\Sigma^*|\cos\gamma - \frac{|\Sigma|}{|\Omega|}|\Omega^*|\cos\gamma - \kappa\int_{\Omega^*} y \,\mathrm{d}x\,\mathrm{d}y > 0. \tag{3.7}$$

Since $\Phi[\Omega] = \Psi[\Omega] = 0$, one finds that $\Phi\left[\Omega^*\right] = \Psi\left[\Omega \backslash \Omega^*\right]$. Thus, *as conditions applying to all subdomains of* Ω *determined by smooth arcs* Γ, (3.6) *and* (3.7) *are*

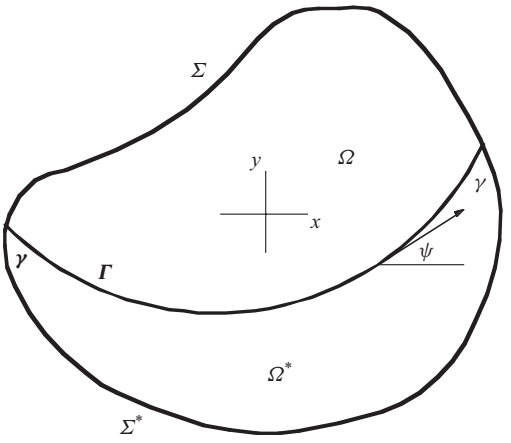

FIGURE 3. General section Ω of cylindrical tube, showing inclination angle ψ on extremal arc $\boldsymbol{\Gamma}$ that meets boundary in angles $\boldsymbol{\gamma}$.

equivalent. We have shown that in the indicated sense, each of these relations is *necessary* for existence of an occluding interface. Thus, *if one can exhibit an Ω^* for which either Φ or Ψ is non-positive, it will follow that there can be no occluding surface.* In this event, some other surface which cannot occlude the tube must presumably exist instead. Cases in which $\Phi > 0$ or (equivalently) $\Psi > 0$ for all subsets Ω^* permit an occluding surface. We make no assertion as to the detailed structure of such surfaces.

As a procedure for determining which of these cases prevails, we observe initially that both Φ and Ψ are bounded below, for any given κ and prescribed Ω. It is thus appropriate to seek minimizing domains for these functionals; *the necessary condition will then be satisfied if and only if each of the functionals is positive on any corresponding minimizing domain.* We approach this problem as in Finn (1986), by writing the Euler–Lagrange equation for the bounding curves Γ of eventual extremal domains. This is the analogue for the present case, of the 'subsidiary extremal problem' introduced in §6.5 of Finn (1986), and which led to the 'nonexistence–existence principle' Theorem 6.8 of that reference.

In suitable local coordinates, as indicated in figure 3, we obtain the equations

$$\frac{\mathrm{d}}{\mathrm{d}x}\frac{y'}{\sqrt{1+y'^2}} = \lambda + \kappa y \tag{3.8}$$

for a Φ extremal, and

$$\frac{\mathrm{d}}{\mathrm{d}x}\frac{y'}{\sqrt{1+y'^2}} = -(\lambda + \kappa y) \tag{3.9}$$

for a Ψ extremal. In both cases, if the extremal intersects Σ, then it does so in the angle γ, measured within Ω^*. In general, there will exist only a finite number of extremals satisfying all these conditions, and thus there will be only a finite number of cases to be examined. Exceptional cases do occur, and must be confronted on their individual merits.

We have limited the above discussion to formal description of the procedure we have used. A more complete discussion of the conceptual background is available in the section on 'Property 5. C-singular solutions' in the expository article of Finn

(2002). Figure 16 of that reference indicates the nature of the transition from occluding surfaces to *soluzioni generalizzate* as the parameters approach critical values.

4. Background remarks

The individual procedures used are best chosen according to the particular problem considered. In general, we may recognize (3.8) and (3.9) as equations for capillary surfaces in a single dimension, with the same solutions for each fixed value of z, see, e.g. §6.5 of Finn (1986). The left sides of (3.8) and (3.9) are the planar curvatures of the arcs $y(x)$, thus imparting a geometrical character to the problem. In the absence of transversal forces, the extremals are circular arcs of known curvature, meeting Σ in the angle γ. The set of all-possible extremals can then, in individual cases, be determined by geometrical considerations, a circumstance that was exploited to striking advantage in earlier literature, cf., some examples described in Finn (1975, 2002).

In the present instance, we obtain the extremals in explicit form by integrating (3.8) and (3.9). Observing that $y'/\sqrt{1+y'^2}$ is the sine of the inclination angle ψ of the extremal Γ with the x-axis, we rewrite these equations in the form

$$\frac{\mathrm{d}\sin\psi}{\mathrm{d}x} = \frac{\mathrm{d}\sin\psi}{\mathrm{d}y}\tan\psi = \frac{\mathrm{d}\psi}{\mathrm{d}y}\sin\psi = \pm(\lambda+\kappa y), \tag{4.1}$$

with positive or negative signs arising, respectively, from (3.8) and (3.9).

The final terms of (4.1) provide separable equations that can be integrated explicitly. For a solution curve through the point (x_0, y_0) with inclination ψ_0 at that point, we obtain, using positive square root

$$y = -\frac{\lambda}{\kappa} + \frac{1}{\kappa}\sqrt{(\kappa y_0+\lambda)^2 \mp 2\kappa\,(\cos\psi_0 - \cos\psi)}. \tag{4.2}$$

We also have

$$\frac{\mathrm{d}x}{\mathrm{d}\psi} = \frac{\mathrm{d}x}{\mathrm{d}\sin\psi}\cos\psi = \pm\frac{\cos\psi}{\lambda+\kappa y} \tag{4.3}$$

by (4.1), so that, again with a positive square root

$$x = x_0 + \int_{\psi_0}^{\psi} \frac{\cos\psi}{\sqrt{(\kappa y_0+\lambda)^2 \mp 2\kappa\,(\cos\psi_0 - \cos\psi)}}\,\mathrm{d}\psi. \tag{4.4}$$

We have incidentally shown that *the function* $(\lambda+\kappa y)^2 \pm 2\kappa\cos\psi$ *is a first integral of (4.1), in the sense that it is constant on any integral curve.*

Although exceptional situations can occur, one expects in general to find only a finite number of curves of the form (4.2) and (4.4) that meet $\Sigma = \partial\Omega$ in the prescribed angle γ. Thus, in general, only a finite number of cases must be tested as to the sign of Φ (or of Ψ).

One sees from (4.2) that $y < y_0 + \sqrt{2/\kappa}$. Thus, *if* y_0 *is chosen negative (below the centroid) and if* κ *is large enough, then* y *will remain below the centroid throughout the traverse, and as a consequence there will hold* $y<0$ *throughout the domain* Ω^* *determined below the extremal.* From this behaviour and (3.6), we then see that if $\Phi[\Omega^*] \leqslant 0$ for such an Ω^* when $\kappa = 0$ then Φ for that same Ω^* will become negative when $\kappa > 0$. We exploit this remark in §6, to design a tube section that will not occlude regardless of gravity.

In general, for the cases that we considered, the precise determination of the extremal arcs Γ turned out to be difficult, and initial configurations were therefore

studied using the SE software of Brakke 2011. This is essentially a 'steepest descent' method, and in a general case one cannot be certain that one achieves a global minimum. However, for simple geometries, one can apply the procedure with some confidence.

5. Example 1: circular pipe

If Ω is circular, the problem adopts a relatively simple form. If gravity vanishes, then occluding surfaces can be found explicitly for any prescribed γ in $0<\gamma<\pi$ as spherical caps, of radius $a/|\cos\gamma|$, where a is the radius of the pipe. Thus continuity considerations suggest that for each γ_0 in that range, there will exist a critical $\kappa_0>0$ such that an occluding surface exists if and only if $\kappa<\kappa_0$.

In principle, we can characterize the dependence $\kappa_0(\gamma_0)$ by finding the solutions (4.2) and (4.4) of (3.8) that meet $\Sigma=\partial\Omega$ in the prescribed angle γ_0, and then evaluate Φ for the domain Ω^* that is cut off by that extremal. This is easy to do in the zero gravity case ($\kappa=0$), in which the extremals are circular arcs of radius $R=a/2\cos\gamma$. It is not hard to show that extremals then exist only for $\gamma>\pi/4$, that these are uniquely determined up to symmetries and that they all yield $\Phi>0$. If $\kappa>0$, we expect a corresponding statement, depending on κ and with Φ becoming negative for κ large; however, the geometrical relations become much more complicated. From the point of view of obtaining concrete results in this case of special interest, we found it technically simpler to minimize numerically the functional Φ using the well-established procedures of the SE software (Brakke 2011). It is important to note that SE is not used in this context to determine the three-dimensional interface shape but rather is used to find the two-dimensional extremal arc. Furthermore, the two-dimensional extremal arc found using SE only minimizes (3.6), and is not necessarily the profile of the non-occluding surface.

In terms of a Bond number

$$B=\frac{\rho g}{\sigma}a^2, \tag{5.1}$$

we may write in coordinates non-dimensionalized with respect to a

$$\Phi\,[\Gamma;\gamma;B]\equiv|\Gamma|-|\Sigma^*|\cos\gamma+2\,|\Omega^*|\cos\gamma+B\int_{\Omega^*}y\,\mathrm{d}\Omega. \tag{5.2}$$

Here, we have used the fact that for the circular pipe, there holds $|\Sigma|/|\Omega|=2/a$. We approximated Γ as a piecewise-linear curve without double points, characterized by 2049 vertices and 2048 edges, joining two distinct points P_1, P_2 of $\Sigma^*$and cutting off a simple domain $\Omega^*\subset\Omega$. Using a 'steepest descent' method, the vertices were translated or 'evolved' to arrive at a lower functional value. Due to the simple geometry, a global minimum exists, and one can apply the procedure with good effect.

Brakke's SE minimizes the functional for a fixed contact angle and Bond number. A simple but fast procedure can be used to find the transition $B=B_0$, at which $\Phi=0$. To prevent SE from finding an empty Ω^*, we must approach B_0 from above. We first choose an initial Γ and take B to be a very large number. The curve is then evolved for a set number of iterations. The Bond number is reduced until the functional is zero. The curve evolution and Bond number adjustment is alternated until the desired precision is achieved.

The accuracy of the results can be verified by calculating the curvature and inclination angle at the wall. The minimizing Γ meets Σ at the contact angle γ within 0.01% at both P_1 and P_2. For a range of contact angles, the transition

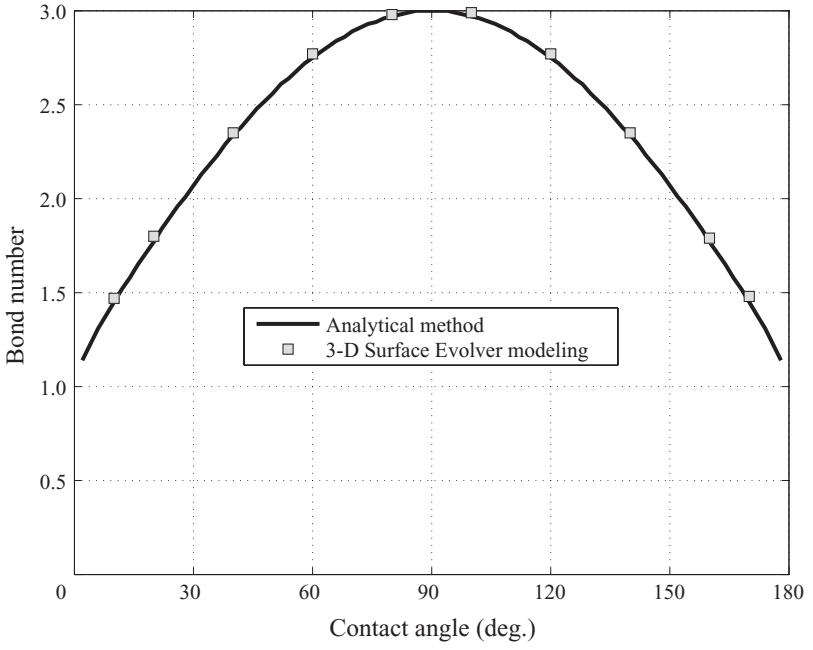

FIGURE 4. Critical Bond number B_0 in terms of contact angle, for circular tube.

values B_0 were calculated. We could determine B_0 approximately within two or more significant figures. The computational time was less than 1 min for each case, thus illustrating the computational efficiency of this method.

Figure 4 compares the analytic theory developed above with direct calculations of the surfaces using Brakke's SE (see comments below) and illustrates the results for all contact angles. If a Bond number is less than B_0, then a bounded solution exists for the capillary problem, and occlusion of the pipe may occur. For values $B > B_0$ occlusion will not occur. Crossing the solid line corresponds to the kind of transition indicated in figure 1, from a smooth solution surface projecting simply onto the section Ω, to a 'soluzione generalizzata' (Giusti 1984) that is identically infinite on a significant subset $\Omega^* \subset \Omega$. The transition can, in some circumstances, occur discontinuously, in the sense that a smooth solution exists at the crossing value $B = B_0$, but that no bounded solution covering Ω exists if $B > B_0$. That behaviour occurs, for example, when Ω is a regular polygon, see, e.g. the discussion in § 6.2 of Finn (1986). The detailed nature of the transition can vary depending on the particular Ω (see § 6.12 of Finn 1986).

The black line consisting of 171 points was computed using the analytic theory presented in this paper. The gray squares were found using Brakke's SE in three-dimensional mode. This was performed by running a series of simulations at different Bond numbers and evaluating convergence. The critical Bond number was found when the surface area increases abruptly for a small change in Bond number. While this numerical procedure is not precisely defined, we found good agreement between the two methods. This point is of practical interest, as there is several orders of magnitude difference in computational efficiency between the methods. Finding B_0 using SE in three-dimensional mode will take several hours on a modern desktop PC. The above procedure to minimize (5.2) requires only a few seconds. Figure 5 displays

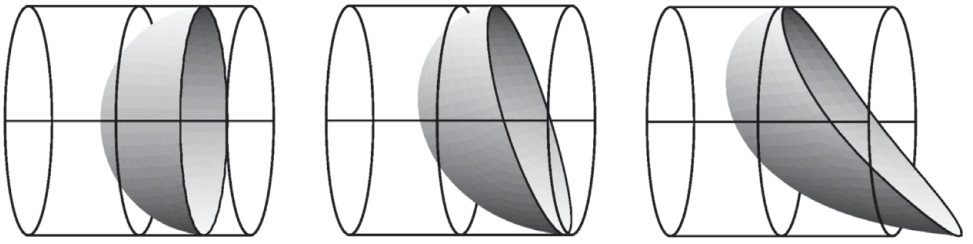

FIGURE 5. Occluding surfaces for $\gamma = 5^\circ$ with $B = 0, 0.5$, and 1.

the actual form of the occluding surface, for $\gamma = 5$ degrees, and for three values of B increasing to the critical Bond number $B_0 \sim 1.25$.

6. Example 2: non-occluding pipe

We consider a cylinder section Ω as a 'flattened ice-cream cone' domain with half-angle α at the vertex, as indicated in figure 6(a). We denote here by 'upper' and 'lower' the increasing or decreasing 'z' directions parallel to the cylinder generators, which we describe as 'vertical'. For a contact angle γ such that $\pi/2 - \alpha \leqslant \gamma < \pi/2$, an explicit solution of (3.1, 3.2, 3.3) with $\kappa = 0$ is obtained as that portion $u(x, y)$ of a lower hemisphere S centred at O and of radius $1/\cos\gamma$, which projects vertically onto the 'horizontally placed' $\Omega(z = c)$; the (c) portion of the figure shows a 'vertical' section of S. The figure indicates the equatorial circle Γ of S in the particular case $\alpha + \gamma = \pi/2$. All larger γ in the indicated range are obtained by increasing the circle radius; in this way, explicit zero-gravity occluding surfaces are obtained, for all γ in that range.

If $\alpha + \gamma < \pi/2$, the above construction fails, as the hemisphere no longer covers all of Ω in vertical projection. In fact, we may introduce a set Ω^* as indicated in figure 7, and compute

$$\Phi(\Omega^*; \gamma; 0) = 2l(\sin\alpha - \cos\gamma) + l^2(\sin\alpha\cos\alpha)/R. \tag{6.1}$$

From $\alpha + \gamma < \pi/2$ follows $\sin\alpha - \cos\gamma < 0$; thus, for sufficiently small l, we obtain $\Phi < 0$, which precludes existence of occluding surfaces in zero gravity.

Additionally, the set Ω^* will lie below the centroid of Ω when l is small enough,; hence, by (3.6) $\Phi[\Omega^*]$ will remain negative with increasing B. We conclude that *for prescribed $\gamma < \pi/2$, a tube section of the indicated shape with $\alpha < \pi/2 - \gamma$ can be relied on to transmit fluids without occlusion regardless of the value of B, provided it is oriented with the point P in the downward direction for the gravity field.* If $\gamma > \pi/2$, an analogous reasoning yields the same result, with the criterion $\alpha < \gamma - \pi/2$.

This result does not depend in an essential way on the presence of a sharp corner at P. One sees easily that the indicated behaviour persists if the corner is rounded by a circular arc of small-enough radius, depending on the magnitude $|\gamma - \pi/2|$. Also, many other types of domain are feasible; for example, a similar reasoning can be applied to a long thin ellipse, oriented so that its major axis is vertical.

We remark here that the restriction above of γ to the range $0 < \gamma < \pi/2$ (wetting fluids) is inessential to the substance of the discussion. In the case of a 'non-wetting' fluid/solid interface for which $\pi/2 < \gamma < \pi$, the criteria $\alpha + \gamma > \pi/2$ ($\alpha + \gamma < \pi/2$) are replaced by $\alpha > \gamma - \pi/2$ ($\alpha < \gamma - \pi/2$). The lower hemisphere S is then replaced by its reflection in the plane of Γ.

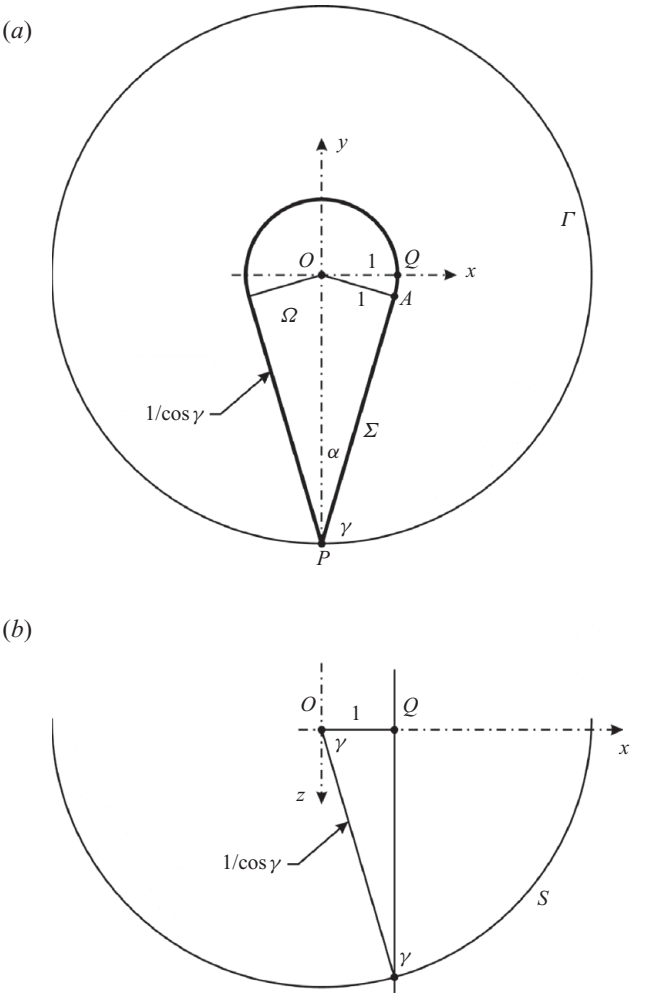

FIGURE 6. (*a*) 'Flattened ice-cream cone' cylinder section Ω; the circular arc on the boundary of Ω extends past Q to A. Equatorial circle Γ of lower hemisphere S meeting cylinder walls Σ in angle $\gamma, \alpha+\gamma=\pi/2$. (*b*) Vertical section of S, through O, showing geometrical relations.

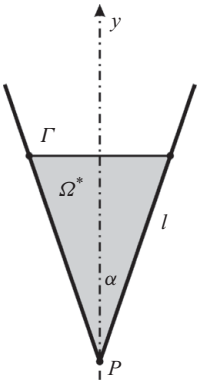

FIGURE 7. Choice of domain Ω^* to obtain $\Phi<0$.

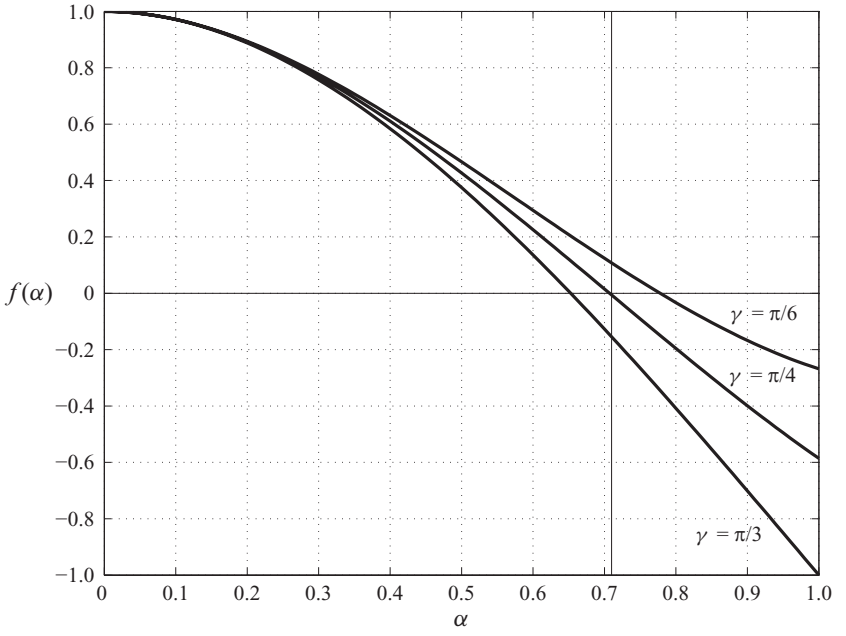

FIGURE 8. $f(\alpha)$ as function of α in the range $0 \leqslant \alpha \leqslant 1$, for three choices of γ. Note that when $\cos\gamma = \sqrt{2}/2$ the critical $\alpha_0 = \sqrt{2}/2$

It should be noted that the above material is complete in itself and does not depend on any general existence theorem. The reasoning depends on the circumstance that in the indicated orientation for the domain with respect to the direction of an eventual gravity field, a necessary condition for existence of an occluding surface is violated independent of the strength of the field. It is, of course, desirable to know that the criterion is sharp, i.e., to know that the necessary condition is also sufficient. That is in fact the case when interpreted properly. For details see Chap. 7 in Finn 1986; that discussion requires some formal extension to encompass the case of transversal fields studied in the present work.

It should not be difficult to construct experiments to test the assertions of this section, as no drop tower should be needed.

7. Example 3 circular centrifuge

In addition to gravitation forces, other body forces can be examined within the framework of this theory. We consider a circular Ω of radius $A > 0$ rotating about its axis at an angular rate ω under weightlessness. We denote by ρ the density of a connected body of liquid filling a linear segment of the tube and rotating rigidly with the tube, and by σ the surface tension of the liquid/air interface. If $\omega = 0$, occluding interfaces can be found as spherical caps of radius $1/|\cos\gamma|$. We seek an $\omega_0 > 0$ such that an occluding surface will exist if and only if $\omega < \omega_0$. The ensuing discussion is complete and mathematically rigorous in the class of symmetric configurations; however, as indicated by figure 9, it presumably applies without that limitation.

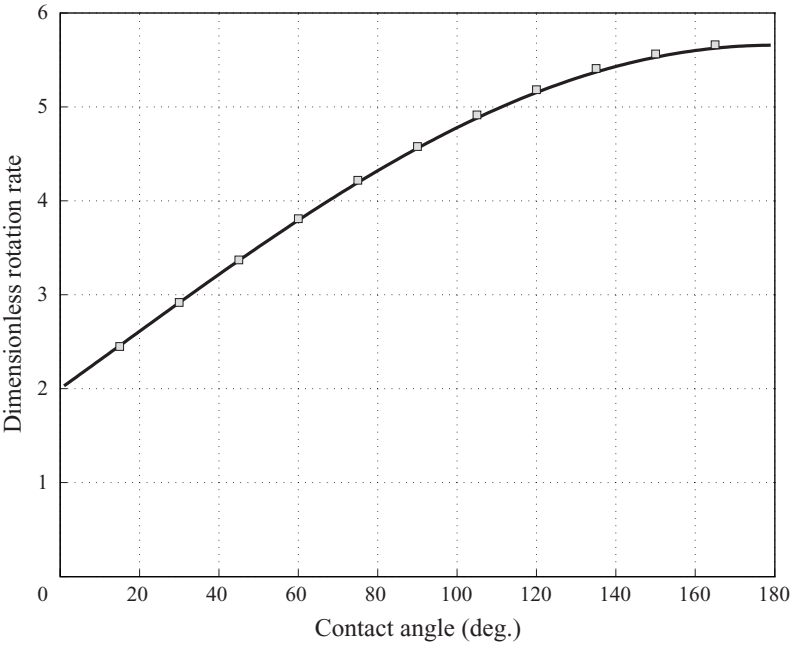

FIGURE 9. Analytical (line) and computational (points) results for critical dimensionless rotation rate for a spinning circular cylinder.

Assuming an occluding surface of the form $u(x, y)$ over the section Ω, the least action principle leads to the equation

$$\mathrm{div} Tu = \frac{1}{2}\frac{\rho\omega^2}{\sigma}(x^2 + y^2) + \lambda, \tag{7.1}$$

where (x, y) are measured from the rotation axis, and λ is a Lagrange parameter arising from a volume constraint. On $\Sigma = \partial\Omega$, we obtain again

$$\nu \cdot Tu = \cos\gamma, \tag{7.2}$$

where γ is the physical contact angle. A discussion analogous to that of § 3 leads to the functional

$$\Phi[\Omega^*; \gamma; \omega] \equiv \sigma\left(|\Gamma| - |\Sigma^*|\cos\gamma + \frac{|\Sigma|}{|\Omega|}|\Omega^*|\cos\gamma\right) + \frac{\rho\omega^2}{4}\left(\pi A^2|\Omega^*| - 2\int_{\Omega^*} r^2\,\mathrm{d}\Omega\right), \tag{7.3}$$

which must be positive for any choice of $\Omega^* \subset \Omega$. We restrict attention to symmetric configurations, and we seek extremal sets yielding $\Phi \leqslant 0$ as concentric subdisks of Ω. Suppose, in fact, that $\Omega^*$is a disk of radius $a < 1$ interior to and concentric with the given disk Ω. Then $\Sigma^* = \emptyset$, and we find thatafter a brief calculation

$$\frac{1}{\pi}\Phi[\Omega^*; \gamma; \omega] = 2\sigma a\left(1 + \frac{a}{A}\cos\gamma\right) + \frac{\rho a^2}{4}\omega^2(A^2 - a^2) \tag{7.4}$$

which is positive for every a in $0 < a < 1$. Thus, (7.4) provides no information that could preclude existence of an occluding surface, and cannot be used to obtain a criterion for existence.

We look instead at the complementary set $\Omega\backslash\Omega^*$, noting that $\Phi[\Omega\backslash\Omega^*;\gamma;\omega]\equiv\Psi[\Omega^*;\gamma;\omega]$, so that, for Ω^* a concentric disk of radius $a<A$, we obtain by analogy with (3.7)

$$\frac{1}{\pi}\Psi[\Omega^*;\gamma;\omega]=2\sigma a\left(1-\frac{a}{A}\cos\gamma\right)-\frac{\rho a^2}{4}\omega^2(A^2-a^2). \tag{7.5}$$

We may write (7.5) in dimensionless form. Setting $\alpha=a/A$, and introducing a 'dimensionless spin rate' $\varpi=\omega\sqrt{\rho A^3/\sigma}$, we consider a new (dimensionless) functional

$$\Upsilon\equiv(1-\alpha\cos\gamma)-\frac{\alpha\varpi^2}{8}(1-\alpha^2), \tag{7.6}$$

which differs from Ψ only by the positive factor $2\pi\sigma a$, and will thus share with Ψ sets of common sign.

We see immediately that the second derivative $\Upsilon_{\varpi\varpi}<0$, with $\Upsilon=0$ attained at the unique value

$$\varpi_0^2=\frac{8}{\alpha}\left(\frac{1-\alpha\cos\gamma}{1-\alpha^2}\right). \tag{7.7}$$

We thus have an explicit criterion ensuring that the tube will not occlude when $\varpi^2\geqslant\varpi_0^2$

In general, Ω^* will not be extremal and (7.7) will not be sharp. Subject to some restrictions, we can, however, choose α so that (7.7) holds and also Ω^* is extremal. We do this most simply by requiring $\partial\Upsilon/\partial\alpha=0$. This yields

$$\varpi_0^2=8\left(\frac{\cos\gamma}{3\alpha^2-1}\right). \tag{7.8}$$

The requirement that (7.7) and (7.8) hold simultaneously yields the equation

$$1-3\alpha^2+2\alpha^3\cos\gamma=0. \tag{7.9}$$

From (7.9), we see that (7.7) and (7.8) can be replaced by the simpler relation

$$\varpi_0^2=4/\alpha^3. \tag{7.10}$$

Denoting the left side of (7.9) by $f(\alpha)$, we find $f(0)=1$, $f(1)=-2(1-\cos\gamma)\leqslant 0$, with equality holding only if $\alpha=\cos\gamma=1$. Also

$$f'(\alpha)=6\alpha(\alpha\cos\gamma-1)<0. \tag{7.11}$$

Thus, *for each* $\cos\gamma$ *in the range* $-1\leqslant\cos\gamma\leqslant 1$, *there is a unique real root* $\alpha(\gamma)$ *of* (7.9) *in an interval* $0\leqslant\alpha*(\gamma)\leqslant\alpha(\gamma)\leqslant 1$; *from* (7.9), *it follows that the correspondence is biunique.*

Setting $\cos\gamma=-1$ in (7.9) yields $(\alpha+1)^2(\alpha-1/2)=0$, and we conclude $\alpha*(\pi)=1/2$. Using (7.10), we see that under all circumstances

$$4\leqslant\varpi_0^2\leqslant 32. \tag{7.12}$$

This estimate cannot be improved; from (7.9) and (7.10), we obtain the explicit value

$$\varpi_0^2=32\sin^3\left(\frac{\pi+2\gamma}{6}\right), \tag{7.13}$$

showing that the lower bound in (7.12) is achieved at $\gamma=0$, the upper one at $\gamma=\pi$.

We observe here that *the radius of an extremal disk is a geometrical constant, independent of the physical parameters* ρ and σ. We note that when $\cos\gamma=0$, there

holds $\alpha = \sqrt{3}/3$, and that when $\cos\gamma = \sqrt{2}/2$, then also $\alpha = \sqrt{2}/2$. The relation (7.9) is illustrated in figure 8, on the interval $0 \leqslant \alpha \leqslant 1$ and $\cos\gamma = 1/2$, $\sqrt{2}/2$ and $\sqrt{3}/2$.

We also find $f''(\alpha) = 6(2\alpha\cos\gamma - 1)$, so that $f''(\alpha) \geqslant 0 \Leftrightarrow \alpha\cos\gamma \geqslant 1/2$.

We find from (7.6) that for any fixed ω

$$\Upsilon_{\alpha\alpha}(\alpha, \varpi) = \frac{3\varpi^2}{4}\alpha > 0 \tag{7.14}$$

for all positive α. Since $\Upsilon(\alpha_0, \varpi_0) = \Upsilon_\alpha(\alpha_0, \varpi_0) = 0$, we obtain that $\Upsilon(\alpha, \varpi_0) > 0$ for all $\alpha > 0$, except for the isolated point $\alpha = \alpha_0$. *We conclude that the original functional Ψ is positive for any circle concentric to the original domain, except for the single disk of radius $a_0 = A\alpha_0$, for which $\Psi = 0$.* This suggests that the configuration is extremal in the sense that $\Psi > 0$ for any domain distinct from the concentric disk of radius a_0.

We have put that assertion to computational test using the SE software. The solid line in figure 9 shows the critical values ϖ_0, as calculated from (7.13). The points on the same figure are determined by the SE in three-dimensional mode, as described in § 2, with some computational effort.

We note that when $\cos\gamma = \sqrt{2}/2$, the extremal configuration is obtained for $\alpha_0 = \sqrt{2}/2$. We show that this configuration corresponds to a qualitative change in behaviour. We examine what occurs

Case 1. $\cos\gamma \geqslant \sqrt{2}/2$. We then have

$$f(\alpha) \equiv 1 - 3\alpha^2 + 2\alpha^3\cos\gamma \geqslant 1 - 3\alpha^2 + \sqrt{2}\alpha^3 \equiv g(\alpha). \tag{7.15}$$

We have $f(0) = g(0) = 1$, $f(1) \leqslant 0$, $g(1) < 0$. Also, $f'(\alpha) = -6\alpha(1 - \alpha\cos\gamma) \leqslant 0$ in the range considered, $g'(\alpha) = -3\alpha(2 - \sqrt{2}\alpha) < 0$. But $g(\sqrt{2}/2) = 0$. We conclude immediately (see figure 8) that $\alpha_0 \geqslant \sqrt{2}/2$.

We can carry the reasoning further. Consider

$$f(\cos\gamma) \equiv 1 - 3\cos^2\gamma + 2\cos^4\gamma \equiv 2(\cos^2\gamma - 1/2)(\cos^2\gamma - 1), \tag{7.16}$$

which vanishes at $\cos^2\gamma = 1/2$ and at 1, and is negative between these values. Suppose first that $\cos\gamma > 0$. Using the result just proven, we find that $f(\alpha_0) = 0 \geqslant f(\cos\gamma)$, with the equality holding only at the two points just indicated. If $\alpha_0 > \cos\gamma$, we would have

$$\int_{\cos\gamma}^{\alpha_0} f'(\xi)\,\mathrm{d}\xi = 0 - f(\cos\gamma) \geqslant 0. \tag{7.17}$$

But $f'(\xi) < 0$, yielding a contradiction. *We conclude that if* $\cos\gamma > 0$, *then* $\alpha_0 < \cos\gamma$, *except at the two endpoints* $\sqrt{2}/2$ *and* 1, *where equality holds.*

Case 2. $\cos\gamma \leqslant \sqrt{2}/2$. Analogous reasoning shows directly that $\cos\gamma \leqslant \alpha_0 \leqslant \sqrt{2}/2$, equality on the left side holding if and only if it holds on the right.

If $\cos\gamma < 0$, then always $\alpha_0 \geqslant 1/2 > \cos\gamma$.

8. Conclusions

We have outlined a general existence/non-existence theory for capillary surfaces over planar domains (sections of a tube of general section) and subject to contact angle boundary conditions in the presence of transverse body forces. We applied the theory to obtain specific criteria determining whether or not a fluid conducting tube of given section can occlude under such a force. We examined in detail three configurations of physical interest, starting with the classical tube of circular section (§ 5), for which we characterized a stability region in terms of the contact angle γ and the

non-dimensional 'Bond Number' for external field strength. The theoretical predictions correlate remarkably with formal calculations using the Brakke SE software.

Our second example (§6) presents the design of a tube that will not occlude when placed horizontally and correctly oriented subject to a downward gravity field, regardless of the strength of gravity. Our criterion here is based on an extension of a zero-gravity non-existence theorem due to Concus and Finn.

As a final example of the procedure, we applied it in §7 to determine a stability criterion for a circular tube containing a plug of liquid in rigid rotation together with the tube, in the absence of gravity. We were led to an explicit upper bound (as formal solution of a cubic equation) for a non-dimensional angular velocity ϖ under which such a configuration can occur. Above that bound, no such fluid 'plug' can exist in rotational equilibrium. Again here we were able to characterize an explicit stability region determined by ϖ and by contact angle, and have found a striking agreement with Surface Evolver calculations.

The theory developed here can be adapted more generally as a procedure for the design of reliable two-phase fluid systems, under varying kinds of applied forces and geometrical constraints.

This work was supported in part by a National Science Foundation Graduate Research Fellowship. The third author (R. F.) thanks the Max-Planck-Institut für Mathematik in den Naturwissenschaften, in Leipzig, for its hospitality and for excellent working conditions during the course of this study. The authors thank P. Concus and A. Yip for helpful remarks.

REFERENCES

Brakke, K. A. 2011 Surface Evolver. http://www.susqu.edu/facstaff/b/brakke/.

Bull, J. 2005 Cardiovascular bubble dynamics. *Crit. Rev. Biomed. Eng.* **33**, 299–346.

Chen, Y. & Collicott, S. H. 2006 Study of wetting in an asymmetrical vane-wall gap in propellant tanks. *AIAA J.* **44**, 859–867.

Collicott, S. H., Lindsley, W. G. & Frazer, D. G. 2006 Zero-gravity liquid–vapor interfaces in circular cylinders. *Phys. Fluids* **18**, 087109.

Collicott, S. H. & Weislogel, M. M. 2004 Computing existence and stability of capillary surfaces using Surface Evolver. *AIAA J.* **42**, 289–295.

Concus, P. 1968 Static menisci in a vertical right circular cylinder. *J. Fluid Mech.* **34**, 481–495.

Concus, P. & Finn R. 1969 On the behavior of a capillary surface in a wedge. *Proc. Natl Acad. Sci.* **63** (2), 292–299.

Concus, P. & Finn, R. 1990 Dichotomous behavior of capillary surfaces in zero gravity. *Micrgravity Sci. Technol.* **3**, 87–92.

Derdul, J. D., Masica, W. J. & Petrash, D. A. 1964 Hydrostatic stability of liquid–vapor interface in low-acceleration field. NASA TN-D-2444.

Finn, R. 1975 On the capillary problem. *Milan J. Math.* **45**, 41–48.

Finn, R. 1986 *Equilibrium Capillary Surfaces.* Springer-Verlag.

Finn, R. 2002. Eight remarkable properties of capillary surfaces. *Math. Intell.* **24** (3) 21–33.

Giusti, E. 1984 *Minimal Surfaces and Functions of Bounded Variation.* Birkhäuser Boston.

Gravesen, P. Branebjerg, J. & Jensen O. S. 1993 Microfluidics – a review. *J. Micromech. Microengng.* **3** (4), 168–182.

Jensen, M., Liebhaber, A., Pelcé, P. & Zocchi, G. 1987 Effect of gravity on the Saffman–Taylor meniscus: Theory and experiment. *Phys. Rev.* A **35** (5), 2221–2227.

de Lazzer, A., Langbein, D., Dreyer, M. & Rath, H. J. 1996 Mean curvature of liquid surfaces in cylindrical containers of arbitrary cross-section. *Microgravity Sci. Technol.* **9** (3), 208–219.

de Lazzer, A., Stange, M., Dreyer, M. & Rath, H. 2003 Influence of lateral acceleration on capillary interfaces between parallel plates. *Microgravity Sci. Technol.* **14**, 3–20.

Litterst, C., Eccarius, S., Hebling, C., Zengerle, R. & Koltay, P. 2006 Increasing uDMFC efficiency by passive CO2 bubble removal and discontinuous operation. *J. Micromech. Microeng*. **16** (9), 248–253.

Masica, W. J. 1967 Experimental investigation of liquid surface motion in respond to lateral acceleration during weightlessness. NASA TN-D-4066.

Reynolds, W. C. & Satterlee, H. M 1966 Liquid propellant behavior at low and zero g. In *Dynamic Behavior of Liquids in Moving Containers* (ed. H. N. Abramsom), NASA-SP-166 1966.

Smedley, G. 1990 Containments for liquids at zero gravity. *Microgravity Sci. Technol.* **3**, 13–23.

Vogel, T. I. 1988 Uniqueness for certain surfaces of prescribed mean curvature. *Pacific J. Math.* **134** (1), 197–207.

Zhang, F. Y. Yang, X. G. & Wang, C. Y. 2006 Liquid water removal from a polymer electrolyte fuel cell. *J. Electrochem. Soc*. **153**, A225–A232.

Zoval, J. V. & Madou, M. J. 2004 Centrifuge-based fluidic platforms. *Proc. IEEE* **92**, 140–153.